GPHS-426

Climatology and *Remote Sensing*

RS Lecture 2

19 December 2023

Remote Sensing (4 X 2-hour classes)

Lecturer: Yizhe Zhan

- Principles of satellite remote sensing (Wed 13 Dec 2023)
- **Meteorological satellites (Tues 19 Dec 2023)**
- Passive remote sensing instruments (Thurs 11 Jan 2024)
- Active remote sensing instruments (Fri 12 Jan 2024)

For course material and hands-on session,

https://github.com/yzhan-met/GPHS-426_RS.git

For reach out for questions, my EDU email is yizhe@illinois.edu.

Outline

1. Recap of the Course 1 - *Principles of satellite remote sensing*
2. Introduction of satellite orbits
3. Constellation of meteorological satellite
4. Drifts and calibration

Basic quantities used in satellite remote sensing

- ✓ Radiance ($\boldsymbol{I_\lambda}$, $\mathrm{W\cdot m^{-2}\cdot sr^{-1}}$) and Irradiance ($\boldsymbol{F_\lambda}$, $\mathrm{W\cdot m^{-2}}$);
- ✓ Volume extinction cross section ($\boldsymbol{\beta_\lambda}$, cm^2), mass extinction cross section ($\boldsymbol{k_\lambda}$, cm^2g^{-1}), and extinction coefficient ($\boldsymbol{\mu_\lambda}$, cm^{-1});
- ✓ Dimensionless quantities such as single scattering albedo ($\boldsymbol{\tilde{\omega}}$), optical depth ($\boldsymbol{\tau}$), and phase function (***P***);

Blackbody radiation laws

- ✓ To calculate the monochromatic flux emitted by a blackbody – Planck function,

$$F_\lambda = \frac{c1}{\lambda^5\left[\exp\left(\frac{c_2}{\lambda T}\right) - 1\right]}$$

- ✓ To calculate the wavelength of maximum emission for a blackbody – Wien's displacement law,

$$\lambda_{max}^{BB} = \frac{2897\ \mu mK}{T}$$

- ✓ To calculate the total flux emitted from a blackbody - Stefan-Boltzmann law,

$$F^{BB} = \sigma T^4$$

Basic radiative transfer equation

- ✓ Without attaching to any coordinate system,

$$\frac{\mathrm{d}I_\lambda}{k_\lambda \rho \mathrm{d}s} = -I_\lambda + J_\lambda$$

Basic radiative transfer equation

- ✓ In a plane-parallel atmosphere,

$$\mu \frac{\mathrm{d}I_\lambda(\tau;\theta,\phi)}{\mathrm{d}\tau} = I_\lambda(\tau;\mu,\phi) - J_\lambda(\tau;\mu,\phi) \tag{4}$$

- ✓ Two special cases,
  - the upward radiance at the top-of-atmosphere (τ=0),

$$I_\lambda(0;\mu,\phi) = I_\lambda(\tau_*;\mu,\phi)e^{-\tau_*/\mu} + \frac{1}{\mu}\int_\tau^{\tau_*} J_\lambda(\tau';\mu,\phi)e^{-(\tau'-\tau)/\mu}\,\mathrm{d}\tau' \tag{5}$$

  - the downward radiance at the surface ($\tau = \tau_*$),

$$I_\lambda(\tau_*;-\mu,\phi) = I_\lambda(0;-\mu,\phi)e^{-\tau_*/\mu} + \frac{1}{\mu}\int_0^{\tau_*} J_\lambda(\tau';-\mu,\phi)e^{-(\tau_*-\tau')/\mu}\,\mathrm{d}\tau' \tag{6}$$

Two approximations to solve radiative transfer equation

- ✓ Single-scattering approximation

$$BRF_\lambda(\mu,\phi;\mu_0,\phi_0) = \frac{\pi I_\lambda(0;\mu,\phi)}{\mu_0 F_\odot} = \tau_* \frac{\widetilde{\omega}}{4\mu\mu_0} P(\mu,\phi;-\mu_0,\phi_0) \tag{7}$$

- ✓ Diffusion approximation

$$F_{\mathrm{dif}} = c_1 e^{-k\tau} + c_2 e^{+k\tau} + \chi\left(\frac{1}{\mu_0^2} - k^2\right) e^{-\frac{\tau}{\mu_0}} \tag{8}$$

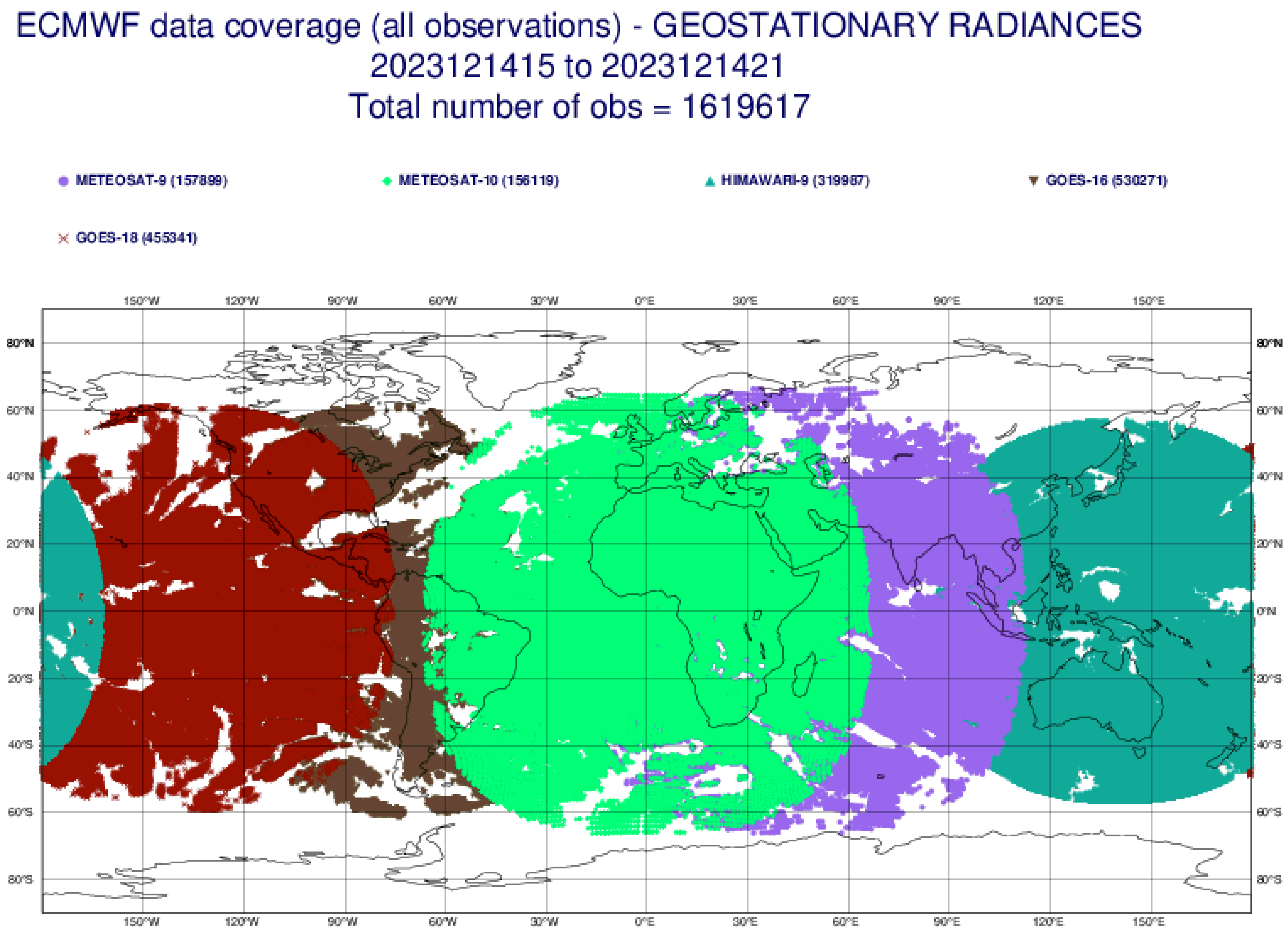
ECMWF data coverage (all observations) - GEOSTATIONARY RADIANCES
2023121415 to 2023121421
Total number of obs = 1619617
METEOSAT-9 (157899)
METEOSAT-10 (156119)
HIMAWARI-9 (319987)
GOES-16 (530271)
GOES-18 (455341)
150°W 120°W 90°W 60°W 30°W 0°E 30°E 60°E 90°E 120°E 150°E
80°N 60°N 40°N 20°N 0°N 20°S 40°S 60°S 80°S

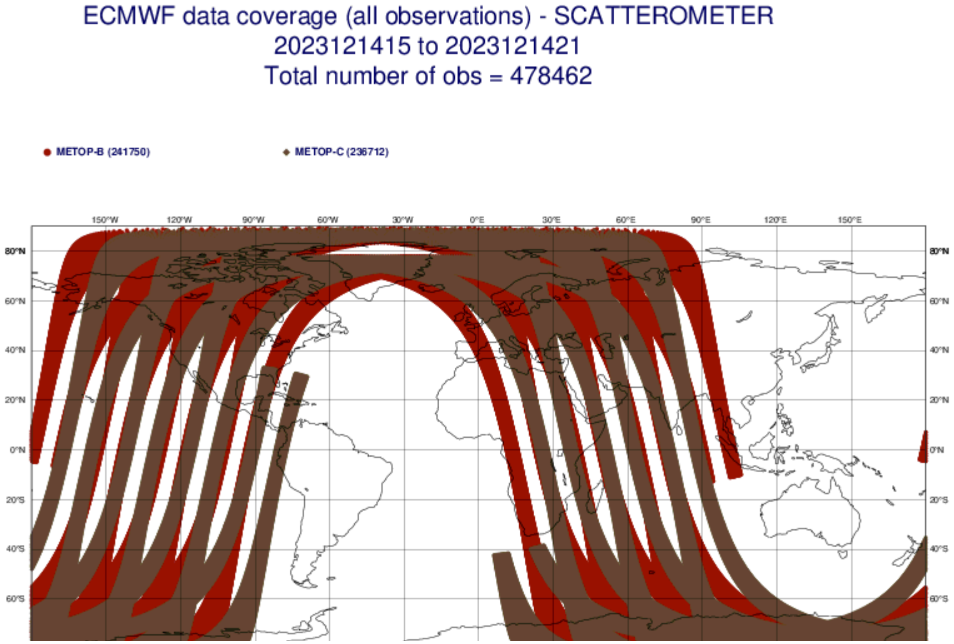
ECMWF data coverage (all observations) - SCATTEROMETER
2023121415 to 2023121421
Total number of obs = 478462
METOP-B (241750)
METOP-C (236712)

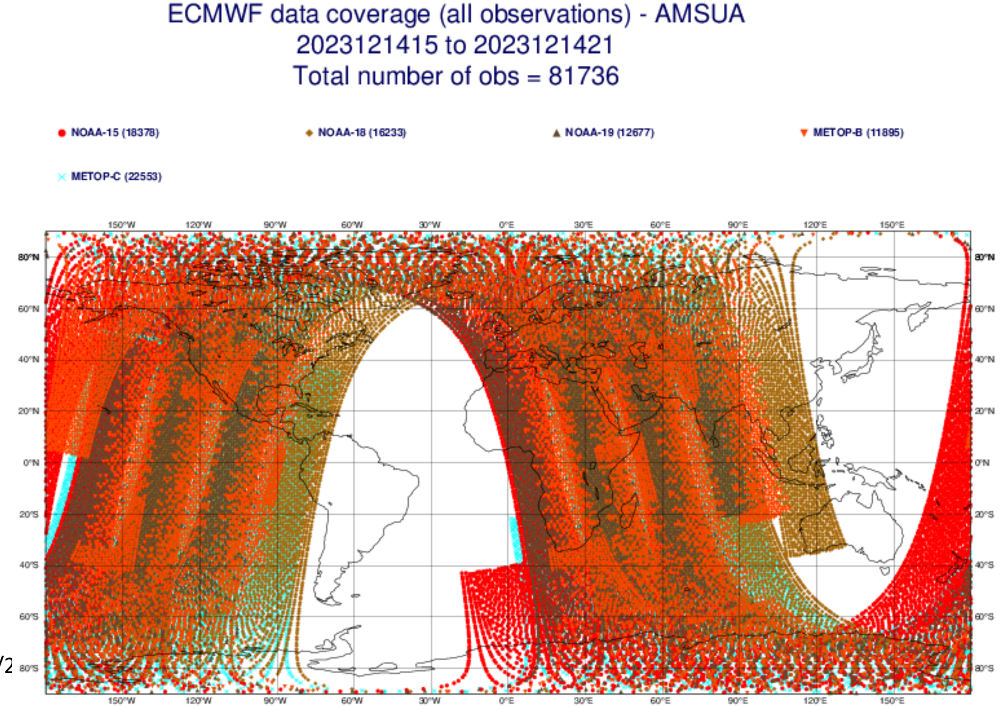
ECMWF data coverage (all observations) - AMSUA
2023121415 to 2023121421
Total number of obs = 81736
NOAA-15 (18378)
NOAA-18 (16233)
NOAA-19 (12677)
METOP-B (11895)
METOP-C (22553)

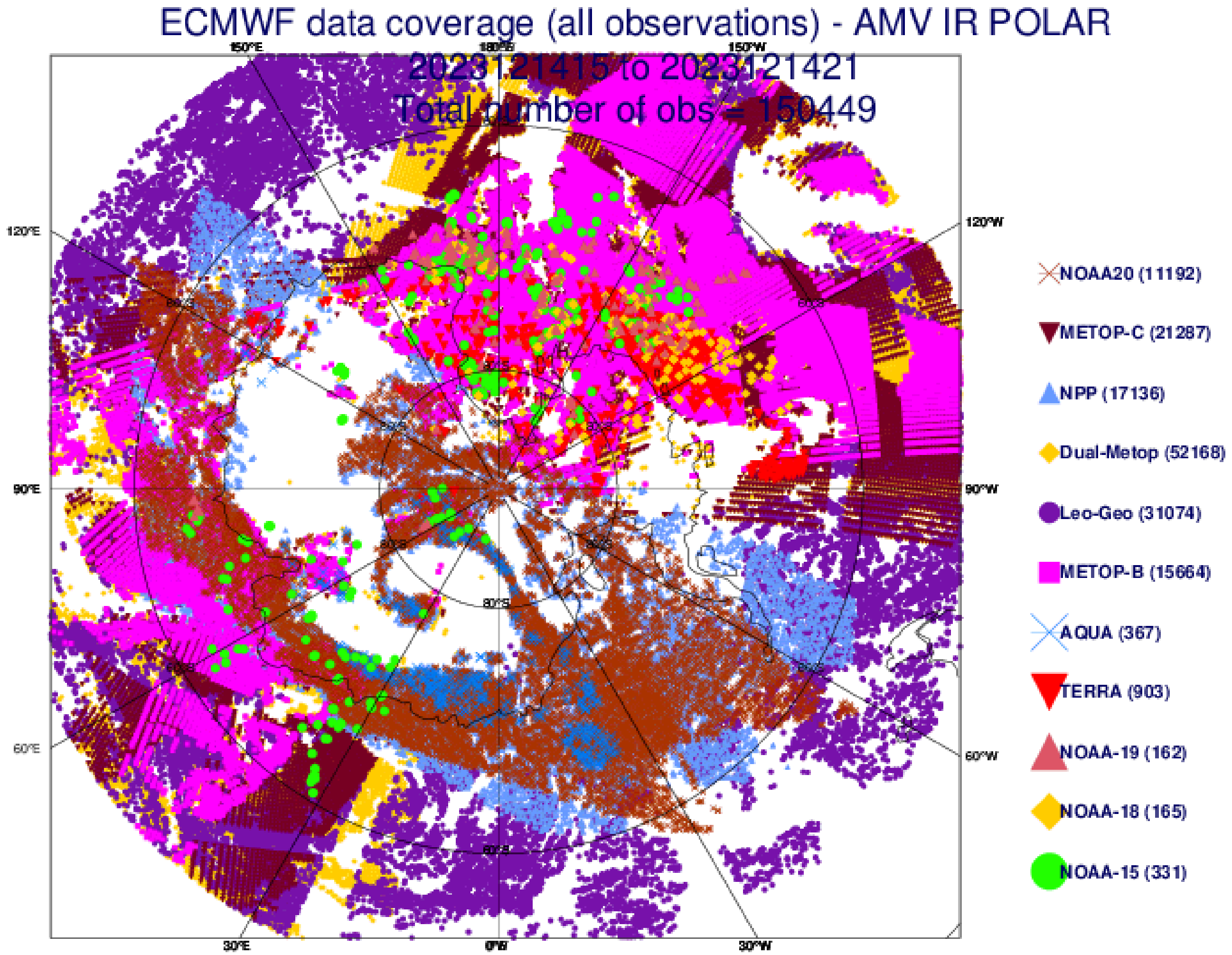
ECMWF data coverage (all observations) - AMV IR POLAR
2023121415 to 2023121421
Total number of obs = 150449
NOAA20 (11192)
METOP-C (21287)
NPP (17136)
Dual-Metop (52168)
Leo-Geo (31074)
METOP-B (15664)
AQUA (367)
TERRA (903)
NOAA-19 (162)
NOAA-18 (165)
NOAA-15 (331)

Three factors

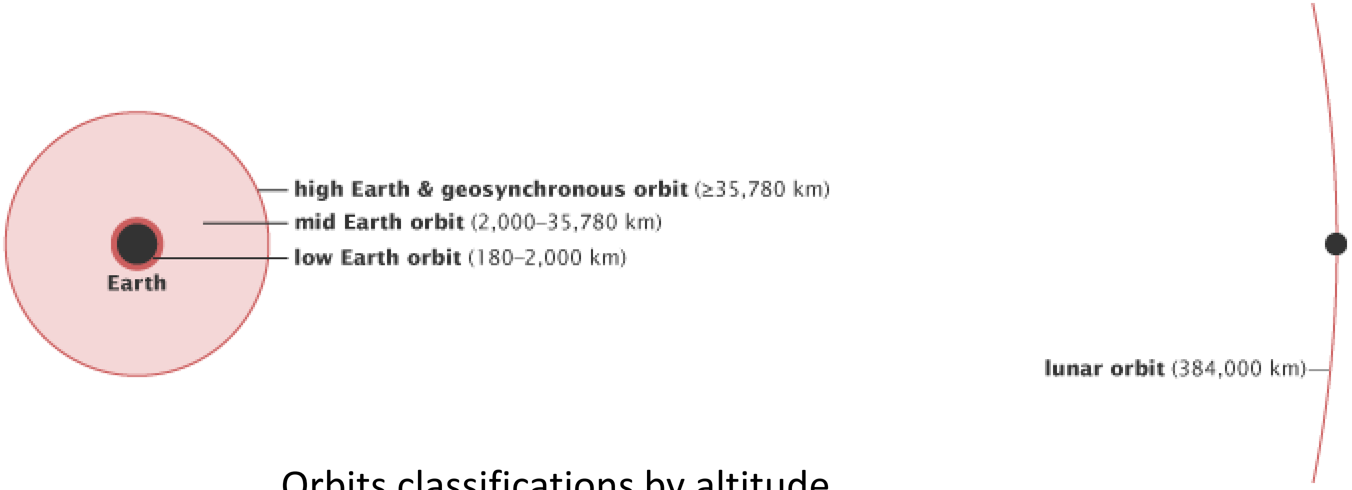

Orbits classifications by altitude

The satellite orbits are shaped by:

- Satellite altitude
- Orbital eccentricity
- Orbital inclination

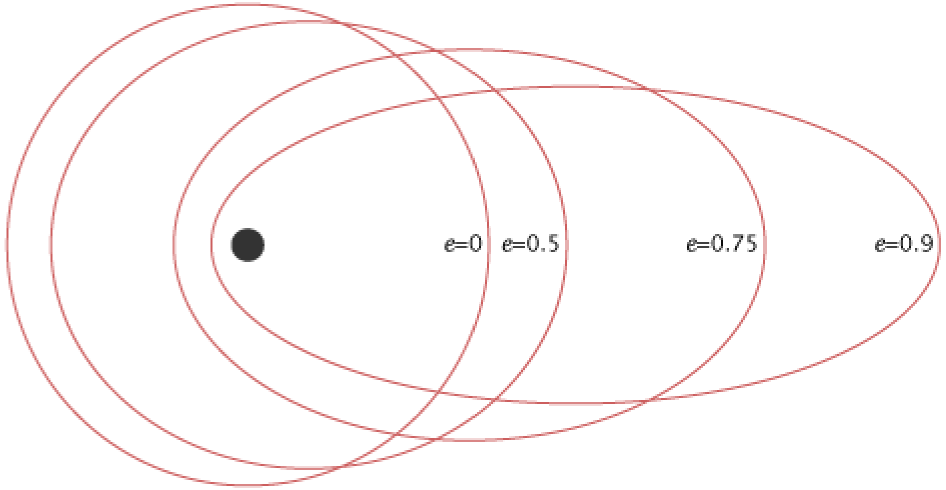

The eccentricity (e) of an orbit indicates the deviation of the orbit from a perfect circle.

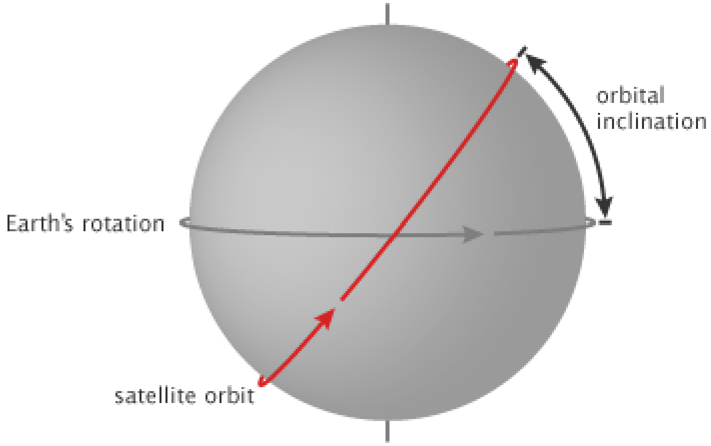

(NASA illustration by Robert Simmon)

Orbits of meteorological satellite

An understanding of satellite orbits is crucial to the understanding of how the various meteorological satellites operate. In this course we will look at two main types of orbit used by operational meteorological satellites. These are:

- Low earth orbit satellites (LEOS)
- Geostationary satellites (GEOS)

We will also briefly discuss other types of satellite orbit, such as the solar orbit. This position allows continuous observation of the sunlit side of the Earth and monitoring of solar wind.

Newton's Laws of Universal Gravitation

Newton's Laws of Universal Gravitation tells us that the attraction force, *F*, between two point masses m_1 and m_2 separated by a distance *r* is

$$F = \frac{Gm_1m_2}{r^2}$$

where G is the universal constant of gravitation, $G = 6.67259 \times 10^{-11}\ \mathrm{Nm^2kg^{-1}}$.

Circular orbits

For a body in circular motion the centripetal force required is

$$F = \frac{mv^2}{r}$$

where v is the orbital velocity of the satellite. The fact that a satellite stays in an orbit around the earth is due to the balance that occurs between the gravitational force and the centripetal force. This balance is also the reason why astronauts and cosmonauts are in a weightless state in space. If we equate the two forces as shown above,

$$\frac{mv^2}{r} = \frac{Gm_em}{r^2} \quad \Rightarrow \quad v^2 = \frac{Gm_e}{r}$$

where m_e is the mass of the Earth, $m_e = 5.9737 \times 10^{24}$ kg. The satellite mass m can be eliminated in the equation.

Low Earth Orbit Satellites (LEOS)

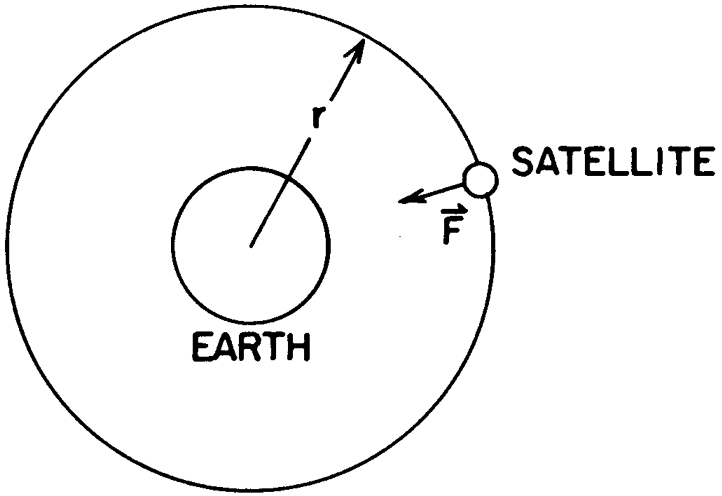

A circular satellite orbit

The circumference of the orbit is $2\pi r$ and if we divide it by the velocity v, we can obtain an expression for the period T, of the orbit

$$T = \frac{2\pi r}{v}$$

square both sides of the equation and then substituting for v^2 in previous equation, we can then have

$$T^2 = \frac{4\pi^2}{Gm_e} r^3 \qquad (1)$$

Let us consider a satellite in a circular orbit 850 km above the Earth's surface. The equatorial radius of the Earth is 6378 km. Therefore, we can substitute this value to obtain an estimate of the period of these satellites,

$$T = \sqrt{\frac{4\pi^2}{Gm_e} r^3} \approx 102 \text{ minutes}$$

The NOAA polar orbit satellites have similar orbital characteristics to this, we will discuss NOAA satellites in detail later.

Low Earth Orbit Satellites (LEOS)

Orbits of (some) operational LEOS

Satellite Name	Regime	Altitude (km)	Inclination (°)	Period (minutes)	Equator Crossing Time
NOAA-20	Sun-synchronous	824	98.7	101	13:30
MetOp-C	Sun-synchronous	817	98.7	101	09:30
Terra (EOS AM-1)	Sun-synchronous	705	98.2	99	10:30
Aqua (EOS PM-1)	Sun-synchronous	705	98.2	99	13:30
Suomi NPP	Sun-synchronous	824	98.7	101	13:30
Fengyun-3C	Sun-synchronous	836	98.7	102	10:00
Copernicus Sentinel-3	Sun-synchronous	814.5	98.65	101	10:00
Copernicus Sentinel-6	Non-sun-synchronous	1336	66	112	Variable
JPSS (Joint Polar Satellite System)	Sun-synchronous	824	98.7	101	13:30
TRMM (Tropical Rainfall Measuring Mission)	Non-sun-synchronous	402	35	92	Variable
GPM (Global Precipitation Measurement)	Non-sun-synchronous	407	65	93	Variable

Differences between SSO and non-SSO

Orbit Type	Altitude (km)	Inclination (°)	Local Solar Time	Purpose	Period (min)	Variability
Sun-synchronous	600 - 800	~98 (nearly polar)	Same part of Earth at roughly the same time daily	Ideal for Earth observation, environmental monitoring, weather satellites	~100 to 120	Consistent solar time for each pass
Non-Sun-synchronous	160 - 2,000	Varies (equatorial to polar)	Various times throughout the day and year	Suited for reconnaissance, scientific experiments, some Earth observation, ISS	~90 to 120	Ground track changes with each orbit

Sun-synchronous and non-Sun-synchronous

Sun-synchronous and non-Sun-synchronous orbits are two different types of orbital paths that satellites use to circle the Earth, each with unique characteristics tailored to specific mission objectives.

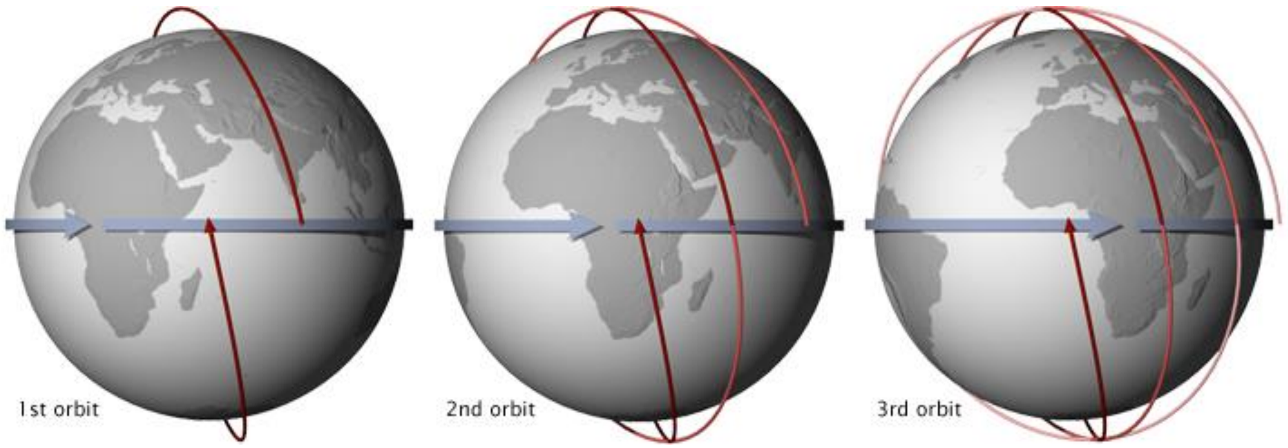

A Sun-synchronous orbit crosses over the equator at approximately the same local time each day (and night). This orbit allows consistent scientific observations with the angle between the Sun and the Earth's surface remaining relatively constant.

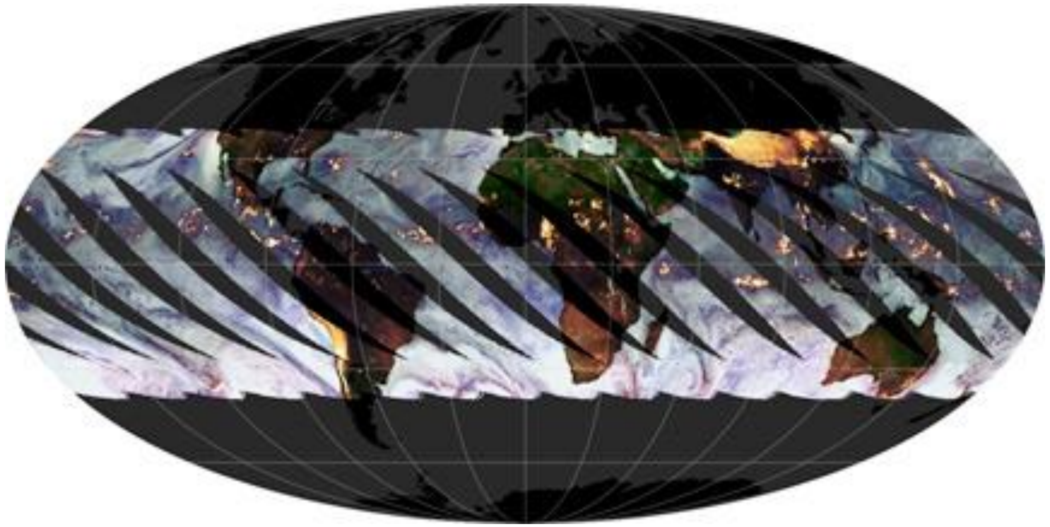

TRMM's low orbital inclination—just 35° from the equator—allows its instruments to concentrate on the tropics. This image shows one half of the observations TRMM makes in a single day.

Sun-synchronous and non-Sun-synchronous

To main a Sun-synchronous orbit, the nodal precession rate must match the Earth's mean motion around the Sun. The nodal precession is caused by the gravitational pull of the Earth's equatorial bulge and can be calculated using the following formula,

$$\omega_p = -\frac{3}{2}\frac{R_E^2}{\left(a(1-e^2)\right)^2} J_2 \omega \cos i$$

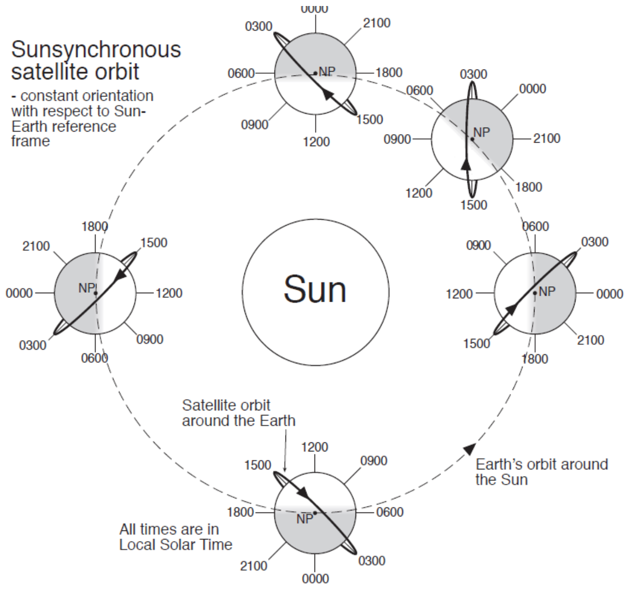

where
ω_p is the precession rate (in rad/s),
R_E is the body's equatorial radius (6378137 m for Earth),
a is the semi-major axis of the satellite's orbit,
e is the eccentricity of the satellite's orbit,
ω is the angular velocity of the satellite's motion,
i is its inclination,
J_2 is the second zonal harmonic of Earth's gravitational field.

For a Sun-synchronous orbit, the precession rate (ω_p) is designed to be approximately 1 degree per day, which is equivalent to the Earth's average daily motion around the Sun (360° per year / 365.2422 days per tropical year ≈ 0.9856473° per day). This keeps the orbital plane in sync with the Earth-Sun line throughout the year.

The precise altitude and inclination values are chosen during mission design to achieve this precession rate and maintain the Sun-synchronous condition.

Low Earth Orbit Satellites (LEOS)

LEOS circle at a low altitude close to the Earth's surface. Their orbits range from 160 km to 2,000 km above Earth but usually fly at an altitude of less than 1,000 km. Because their plane can be tilted, they can fly different routes around Earth - they are most commonly used for satellite imaging because they can take images of higher resolution. It takes them approximately 90 to 120 minutes to circle Earth and complete 12 to 16 orbits per day.

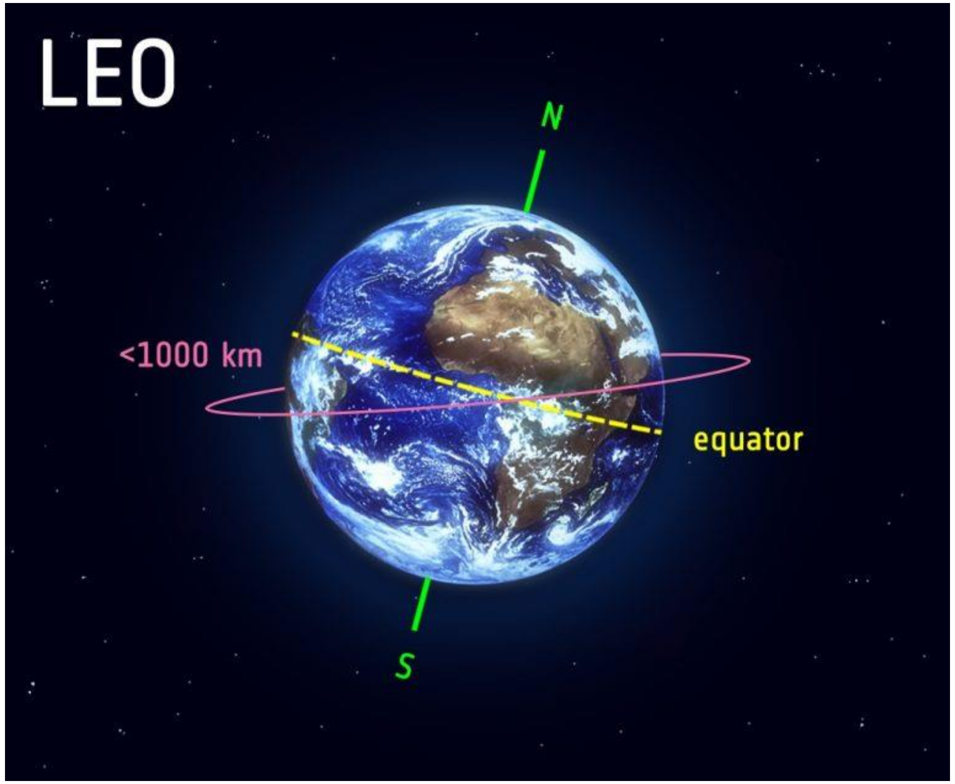

Advantages of LEOS

- Much lower latency for data acquisition (than GEOS);
- Provide more detailed images because of the low orbits;
- Provide excellent views of the polar regions;
- Much higher spatial resolution at cost of a narrower FOV;
- Lower costs to build;

Disadvantages of LEOS

- Cannot see the entire surface of the Earth at once;
- LEOS must relay their data through other satellites in order to reach ground stations;
- Their lifespan is much shorter. LEO satellites have a lifetime of 7-10 years.
- Unable to give near real-time detections due to their high revisit times.

Geosynchronous Satellites (GEOS)

OSCAR
Observing Systems Capability Analysis and Review Tool

Home | Observation Requirements | Space-based Capabilities | Surface-based Capabilities
Overview | Programmes | Satellites | Instruments | Frequencies | Agencies | Satellite Status | Gap Analyses

Satellite: Himawari-9

Satellite details

Acronym	Himawari-9		
Full name	Himawari-9		
Satellite Description	• 2nd flight unit of the Himawari 3rd generation programme. • Main mission: operational meteorology. • Additional mission: environmental applications		
Mass at launch	3500 kg	Dry mass	1300 kg
Power	2600 W		
Data access link	http://www.jma.go.jp/jma/jma-eng/satellite/dissemination.html		
Data access information	• Near-real time availability of AHI images and DCP messages through Internet Cloud service (only for National Meteorological Services) • HimawariRequest to ask for rapid repeat over target area here • Dissemination of reduced resolution AHI data on HimawariCast, see here		
Orbit	Geostationary orbit	Altitude	35786 km
Longitude	140.7° E		

Space agency	JMA		
Status	Operational		
Details on Status (as available)	Himawari-9 replaced Himawari-8 as primary on 13 Dec 2022.		
Launch	02 Nov 2016	EOL	≥2030
Last update:	2023-10-02		

By rearranging $T = \sqrt{\frac{4\pi^2}{Gm_e} r^3}$, we can estimate the height of the orbit of GEO satellite,

$$r = \sqrt[3]{\frac{Gm_e}{4\pi^2} T^2}$$

The Earth completes one revolution in 1 sidereal day which equals 23 hours 56 minutes 4.1 seconds or 86,164.1 seconds (NOTE not 24 hours). If we use the angular velocity $\xi = \frac{2\pi}{T}$, of the Earth, r is then given as

$$r = \sqrt[3]{\frac{Gm_e}{\xi^2}}$$

ξ is equal to $7.292115 \times 10^{-5}\ \mathrm{s}^{-1}$, so we can estimate the height of the GEO orbits $r = 42164\ \mathrm{km}$. By subtracting the Earth radius of 6378 km from r, the satellite is 35786 km above the Earth's surface.

Despite the simple calculation, it gives a very good estimate of the actual altitude of the GEO satellite (e.g., Himawari-9).

Geosynchronous Satellites (GEOS)

Orbits of (some) operational GEOS

Satellite Name	Agency	Launch Date	Altitude (km)	Sub-satellite Longitude	Note
GOES-16 (GOES-East)	NOAA	Nov 2016	35,786	75.2° W	Covers North America, Atlantic Ocean
GOES-17 (GOES-West)	NOAA	Mar 2018	35,786	137.2° W	Covers North America, Pacific Ocean
Meteosat-10	EUMETSAT	Jul 2012	35,786	0°	Covers Europe, Africa
Meteosat-9	EUMETSAT	Dec 2005	35,786	45.5° E	Covers Europe, Africa, Indian Ocean
Himawari-9	JMA	Nov 2016	35,786	140.7° E	Covers East Asia, Western Pacific
Electro-L No.2	Roshydromet/ROSCOSMOS	Dec 2015	35,786	76° E	Covers Russia, Eurasia
Fengyun-4A	CMA	Dec 2016	35,786	86.5° E	Covers China, Asia
GEO-KOMPSAT-2A	KMA	Dec 2018	35,786	128.2° E	Covers East Asia, Western Pacific
Insat-3DR	ISRO	Sep 2016	35,786	74° E	Covers India, Indian Ocean

Geosynchronous Satellites (GEOS)

GEOS orbit the Earth at a much higher altitude than LEOs at about 35,800 km (22,300 miles) above Earth's equator at the speed and direction equal to Earth's rotation, which means they maintain their positions at a fixed longitude, enabling them to provide frequent repeat full disk imagery every 5 – 15 minutes. A single geostationary satellite can see 42% of the earth's surface, and a constellation of three equally spaced geostationary satellites can provide approximately 80% coverage of the Earth at once because they are limited to the curvature of the Earth.

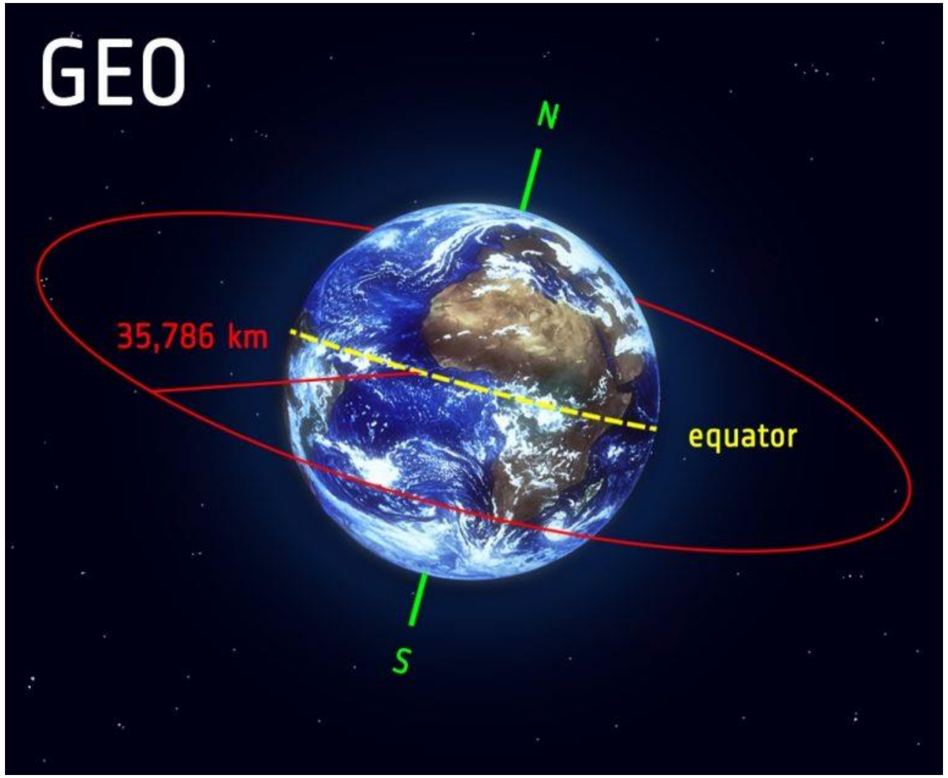

Advantages of GEOS

- Have a full view of planet Earth at all times;
- Can take pictures as frequently as once per minute;
- Allow for continuous monitoring of a specific region;
- Have much higher data transmission rates and less susceptible to atmospheric interference than their low-Earth and polar-orbiting counterparts.

Disadvantages of GEOS

- Lower detailed view because of the high altitude;
- Limited views of the polar regions because of the Earth curvature;
- More susceptible to debris collisions because of the stationary orbit;
- Have a relatively low spatial resolution;
- More expensive to build and launch.

Solar orbit satellite

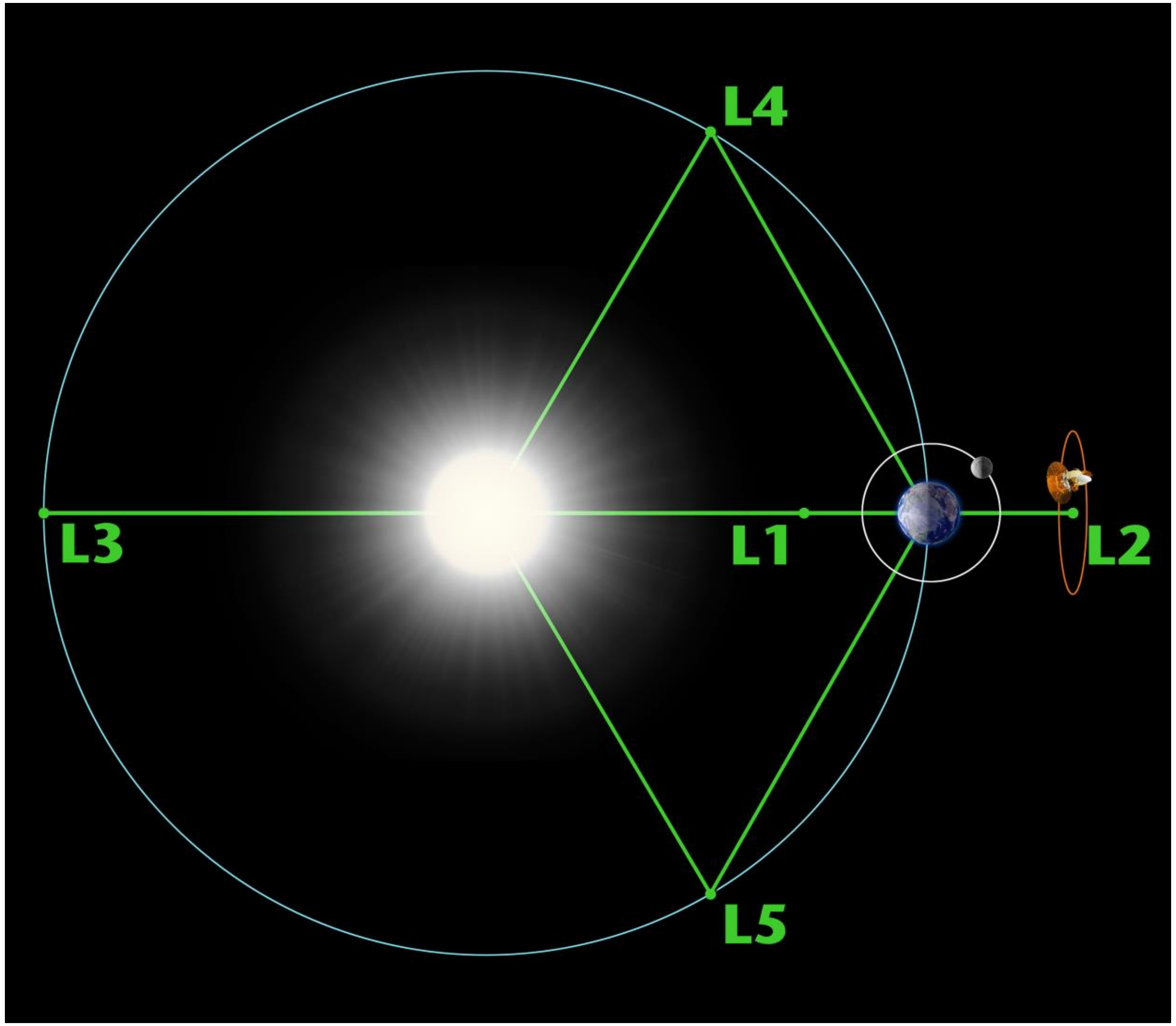

The Deep Space Climate Observatory (DSCOVR) satellite, unlike traditional Earth-orbiting satellites, is positioned at the Lagrange point L1.

- The L1 point is one of the five Lagrangian points in the Sun-Earth system, where the gravitational forces of the Earth and the Sun, along with the orbital motion of the satellite, create a point of equilibrium.
- Satellites that orbit the Sun rather than Earth.
- In practice, the DSCOVR satellite is not exactly at L1 point, as it can orbit around L1 and will require occasional adjustments to maintain its position.

Solar orbit satellite

The ESA telescope Gaia orbits around an L-2 point. The point is exactly behind Earth, so at this point Gaia would be in Earth's shadow and unable to receive the sunlight needed to power its solar panels. Every few years, Gaia uses its motors to adjust its position in order to maintain this orbit.

Solar orbit satellite

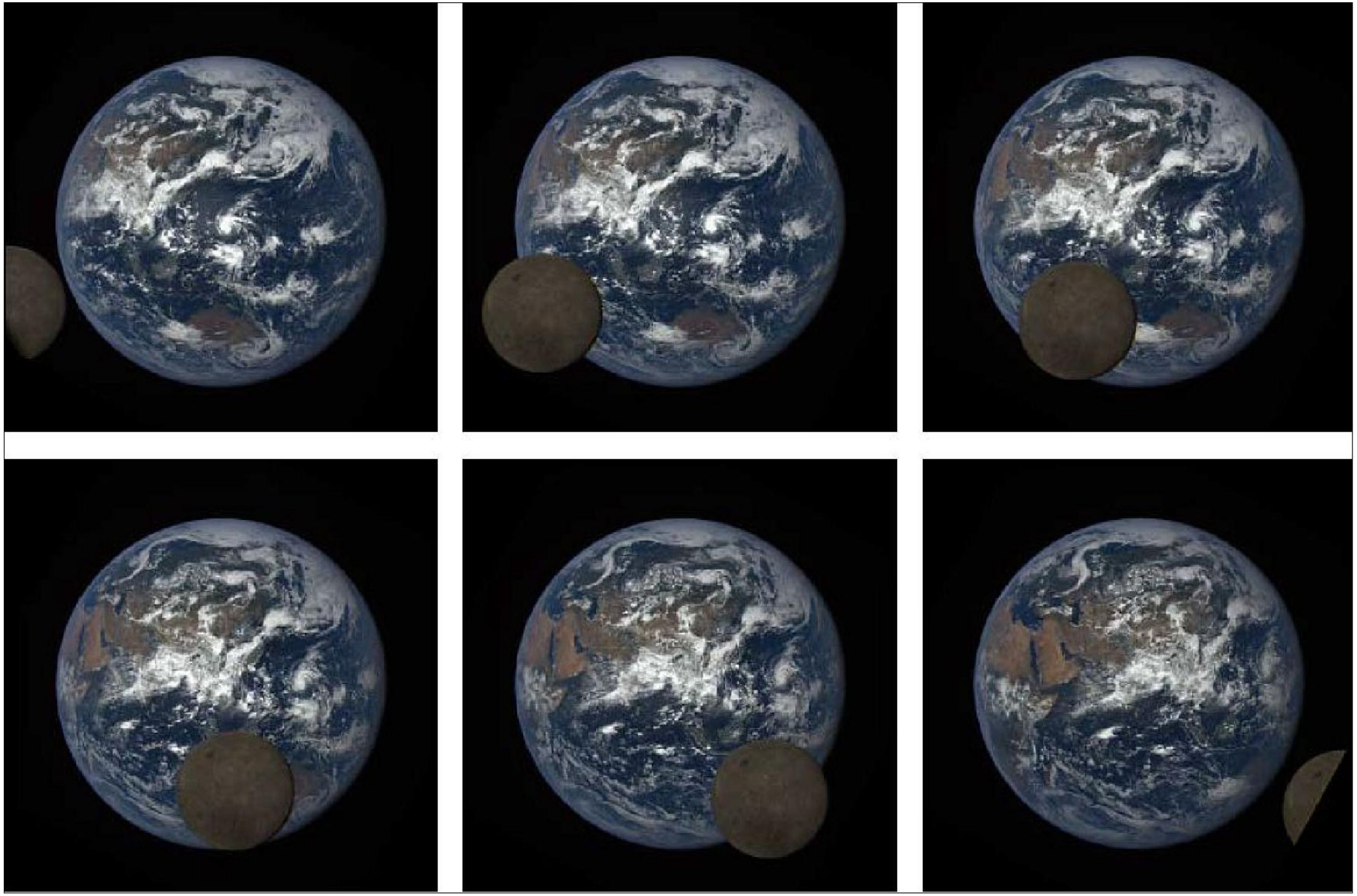

(image credit: NASA)

Molniya orbit satellite

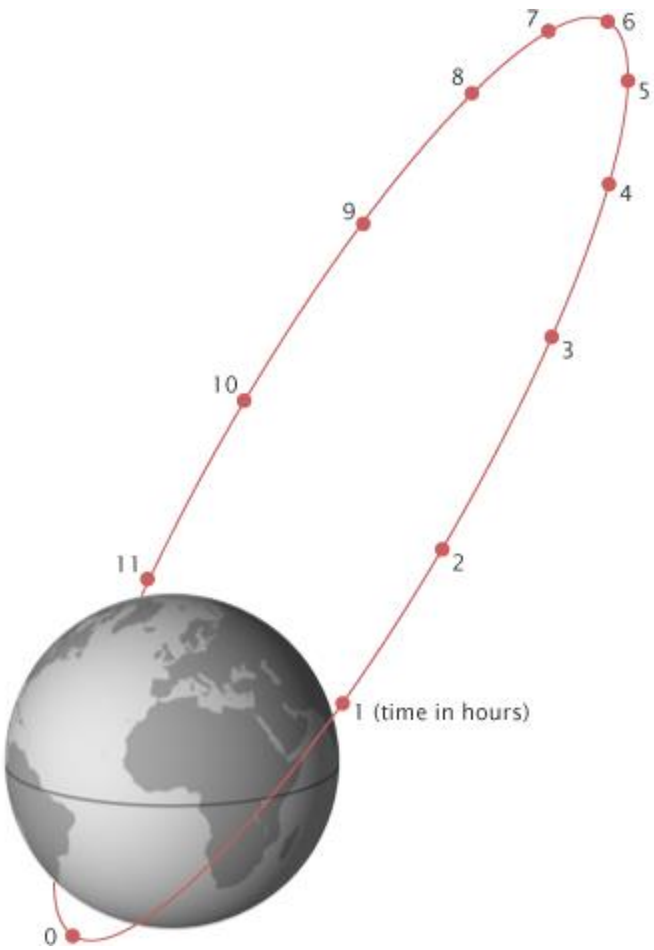

Belong to the Medium Earth Orbit, the Molniya orbit combines high inclination (63.4°) with high eccentricity (0.722) to maximize viewing time over high latitudes.

- The Molniya orbit is highly eccentric - the satellite moves in an extreme ellipse with the Earth close to one edge.
- A satellite in a Molniya orbit takes 12 hours to complete its orbit, but it spends about two-thirds of that time over one hemisphere.
- This type of orbit is useful for communications in the far north or south.
- The Molniya orbit offers a useful alternative to the geostationary orbit.

(Adapted from Fundamentals of Space Systems by Vincent L. Pisacane, 2005.)

To sum up

- Most of meteorology satellites fly in two different types of orbit. For example, at EUMETSAT, the Meteosat satellites fly in a geostationary orbit (GEO), while the polar orbiting Metop satellites fly in a sun-synchronous low Earth orbit (LEO).
- A geostationary satellite is positioned above the Equator and orbits the Earth at the same rotation speed as the Earth itself, making it appear stationary from the point of view of an observer on the Earth’s surface. It flies very high above the surface of the Earth, and thus is able to capture the whole Earth disc at once.
- A polar orbiting satellite circles the Earth at a near-polar inclination, meaning that it always passes almost exactly above the poles. The satellite passes the equator and each latitude at the same local solar time each day, meaning the satellite passes overhead at essentially the same solar time throughout all seasons of the year. The low Earth orbit is much closer to Earth than a geostationary orbit, and thus can see a smaller part of the Earth below than a geostationary satellite, but in finer detail.
- The two types of weather satellite, polar and geostationary, should be seen as complementary. Each type has advantages and disadvantages, and an ideal observing system combines both elements.

(image credit: NASA)

Using constellations of satellites rather than relying on a single satellite offers several significant advantages, particularly for applications that require comprehensive coverage and data reliability:

1. Improved Coverage & Temporal Resolution
2. Redundancy
3. Data Richness and Diversity
4. Cost Efficiency
5. Focused Specialization
6. Continuous Development
7. Scalability

GEOS constellations

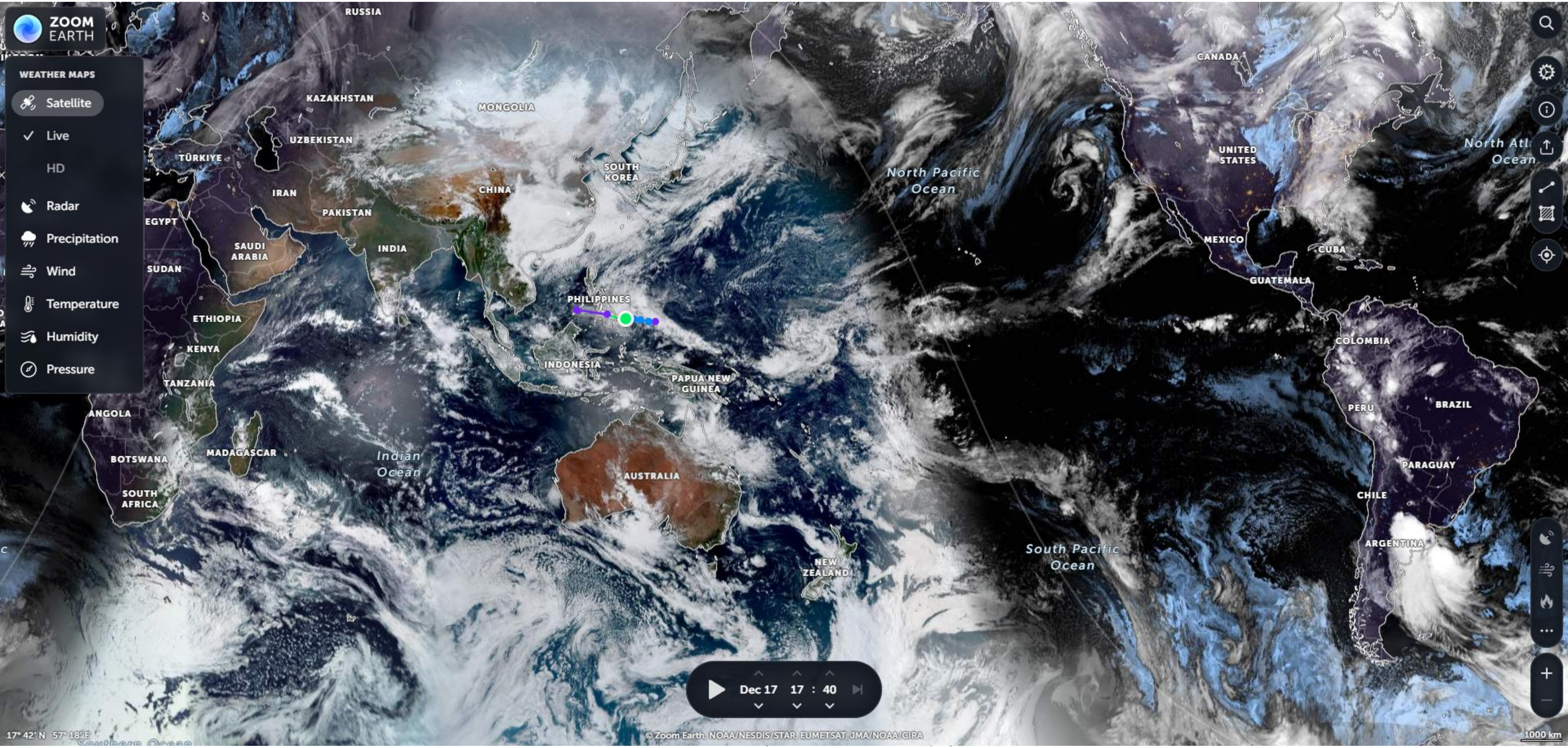

A-Train constellation

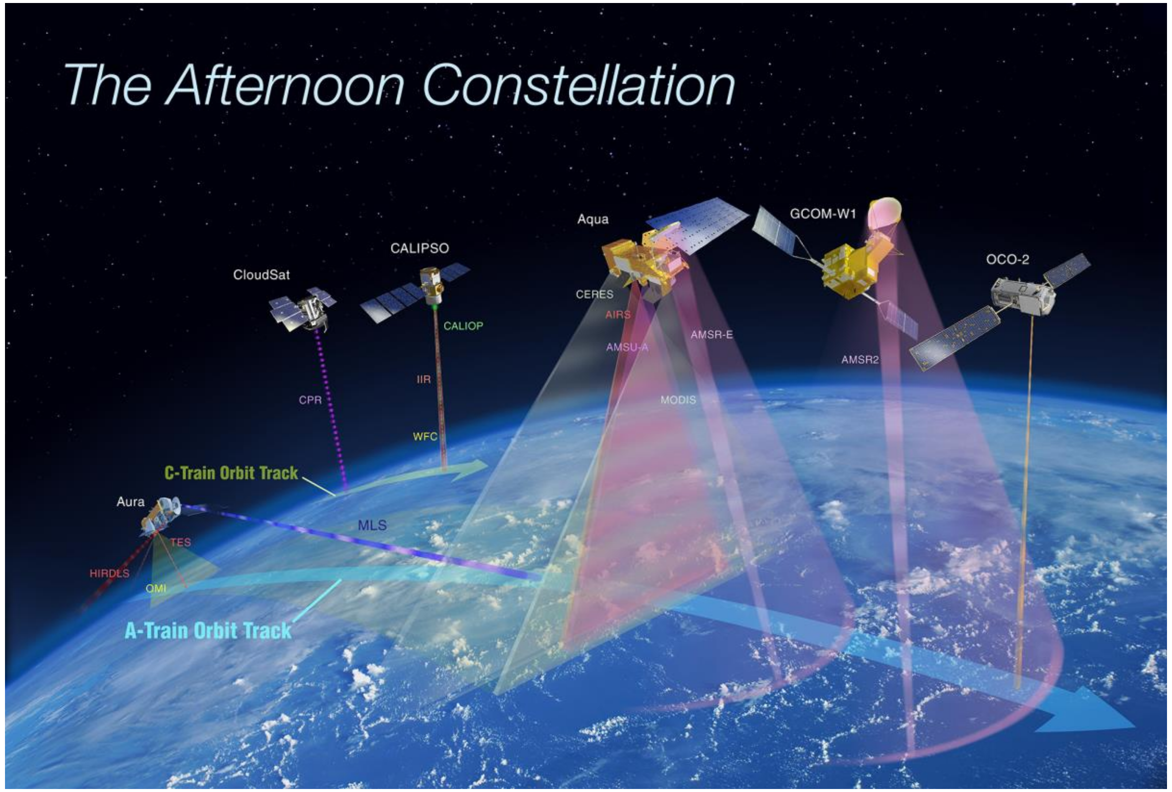

The A-Train (Afternoon Train) constellation is a group of international Earth observation satellites that fly in formation in a sun-synchronous orbit. This constellation is known as the A-Train because the satellites cross the equator at approximately 1:30 PM local solar time.

Satellites fly near one another, which allows for simultaneous collection of data about the same swath of Earth from different perspectives.

Satellites carry a variety of instruments that measure many different properties of the Earth's atmosphere, oceans, and surface.

Notable satellites that have been part of the A-Train include Aqua, **CloudSat**, **CALIPSO** (Cloud-Aerosol Lidar and Infrared Pathfinder Satellite Observations), **PARASOL** (Polarization and Anisotropy of Reflectances for Atmospheric Sciences coupled with Observations from a Lidar), **Aura**, **Aqua,** and the Orbiting Carbon Observatory-2 (**OCO-2**).

Provide synergistic measurements by combining the data from the various instruments across the constellation.

The constellation enables long-term environmental monitoring, which is critical for understanding changes in the Earth’s climate system.

GPM constellation

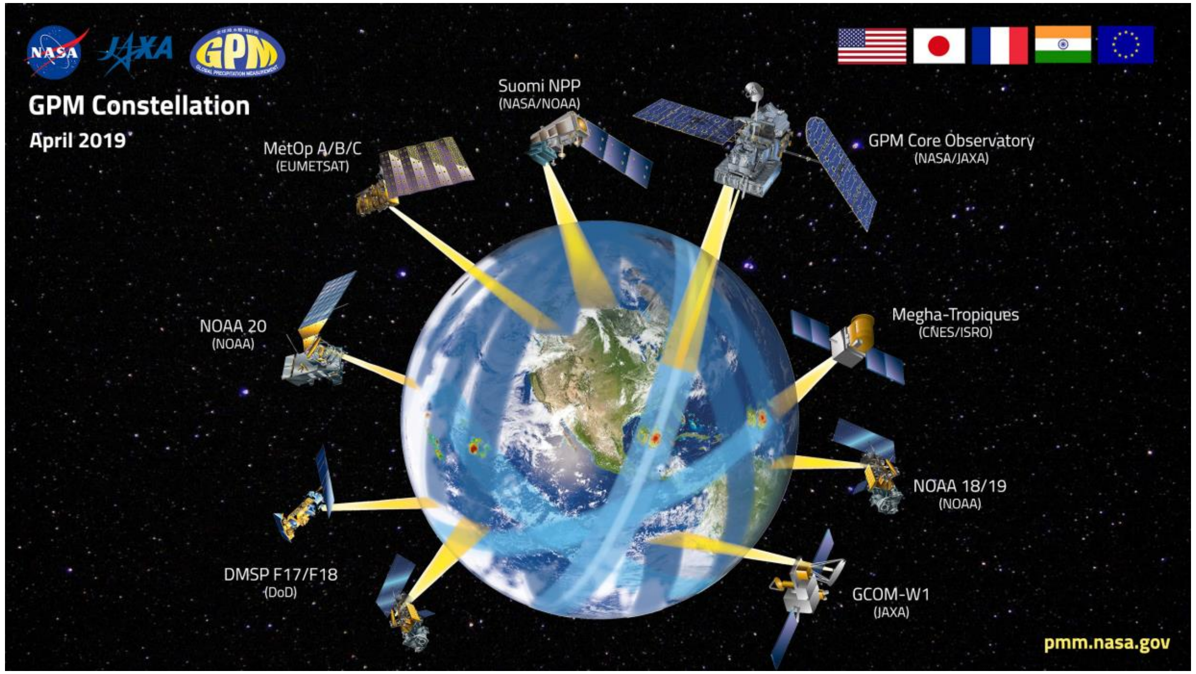

The Global Precipitation Measurement (GPM) constellation is an international network of satellites that provides next-generation global observations of rain and snow. The core of this mission is the GPM Core Observatory, a satellite co-developed by NASA and JAXA.

GPM serves as a successor to the Tropical Rainfall Measuring Mission (TRMM), providing continuity and enhancement of precipitation data crucial for climate monitoring and research.

The GPM Core Observatory carries advanced radar and radiometer instruments that set new standards for precipitation measurements from space, providing detailed observations of the three-dimensional structure of precipitation events.

The GPM Core Observatory is supplemented by a fleet of additional satellites provided by international partners, which contribute diverse precipitation measurements that enhance the global coverage and data accuracy.

The GPM constellation achieves near-global coverage, extending from the Arctic Circle to the Antarctic Circle.

The constellation provides precipitation measurements at high temporal frequencies, often with observations of the same location every few hours.

JPSS constellation

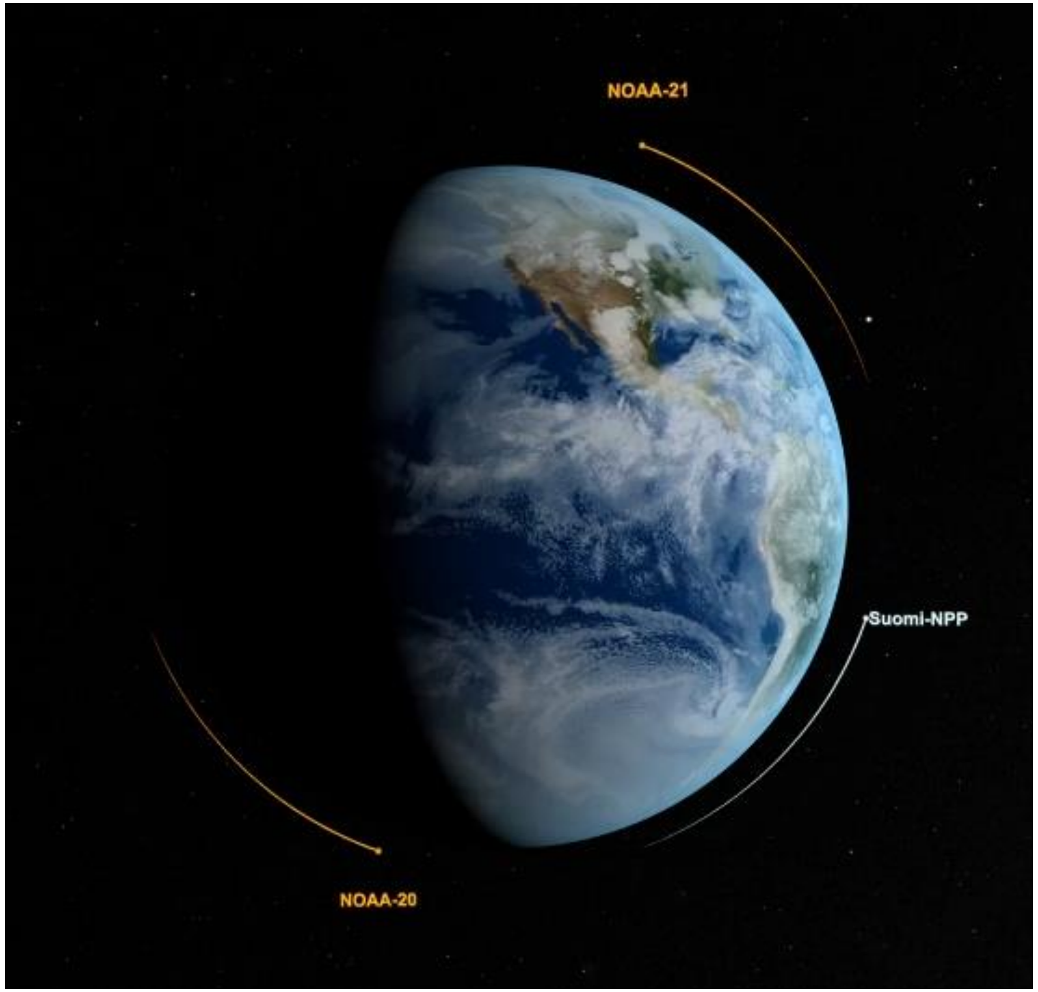

The JPSS (Joint Polar Satellite System) is designed to provide global environmental data critical for public safety, weather forecasting, climate monitoring, and environmental stewardship.

JPSS satellites operate in a sun-synchronous orbit about 824 kilometers above the Earth.

It includes five satellites, the currently-flying NOAA/NASA Suomi National Polar-orbiting Partnership (Suomi NPP) satellite, NOAA-20, NOAA-21, and the upcoming JPSS-3 and JPSS-4 satellites.

The satellites carry a suite of advanced instruments that provide high-resolution data for weather prediction and environmental monitoring. These instruments include the Advanced Technology Microwave Sounder (**ATMS**), the Cross-track Infrared Sounder (**CrIS**), the Visible Infrared Imaging Radiometer Suite (**VIIRS**), and the Ozone Mapping and Profiler Suite (**OMPS**).

The JPSS constellation, along with international partners' satellites, ensures the continuation of observations in the afternoon orbit, providing a global observation every 12 hours.

Station-keeping and instrument calibration are critical factors that can significantly impact the quality and reliability of data collected by weather satellites.

1. **Data Accuracy** - Calibration drift in sensors can lead to systematic measurement errors, affecting the accuracy of weather observations and forecasts.
2. **Data Consistency** - Orbital drift alters the satellite's overpass times, affecting the temporal resolution and consistency of the data, which is crucial for tracking weather systems and long-term climate analysis.
3. **Algorithm Validation** - Inaccuracies in calibration can disrupt the performance of algorithms used for processing and interpreting satellite data, leading to less reliable weather and climate predictions.
4. **Climate Monitoring** - Long-term climate studies depend on stable, well-calibrated satellite measurements. Calibration drift over time can compromise the quality of climate data records, impacting our understanding of climate change trends.

Perturbation of satellite orbits

A number of perturbing forces exist to impact the satellites travelling in their orbits,

Forces which perturb satellite orbits

Force	Size relative to g	Comment
Direct Gravity	1	
Oblateness of the earth	10^-2	Due to bulge at equator, (J_2)
Friction (150 to 1000km)	10^-4	Depends on aerodynamics and altitude
Irregularity in shape of earth	10^-3	Regional density contrasts on earth
Gravitational attraction of Moon	10^-5	
Gravitational attraction of Sun	10^-5	
Solar radiation pressure	10^-6	Solar radiation in sunlit part of orbit
Forces originating from satellite	variable	Orbital correction systems, etc.

The relative strengths of these forces vary and can depend on the height and type of the satellite orbit. For example, the geostationary satellites which orbit high above the earth are not affected by atmospheric drag whereas for low orbiting satellites drag can be significant.

Of the forces listed in Table, the effect of the non-spherical earth is the most predictable and easiest to deal with. The other forces are relatively minor, but less predictable. During the operational lifetime of a satellite, its position is accurately monitored and maneuvered to correct changes in the orbit.

Perturbation of satellite orbits

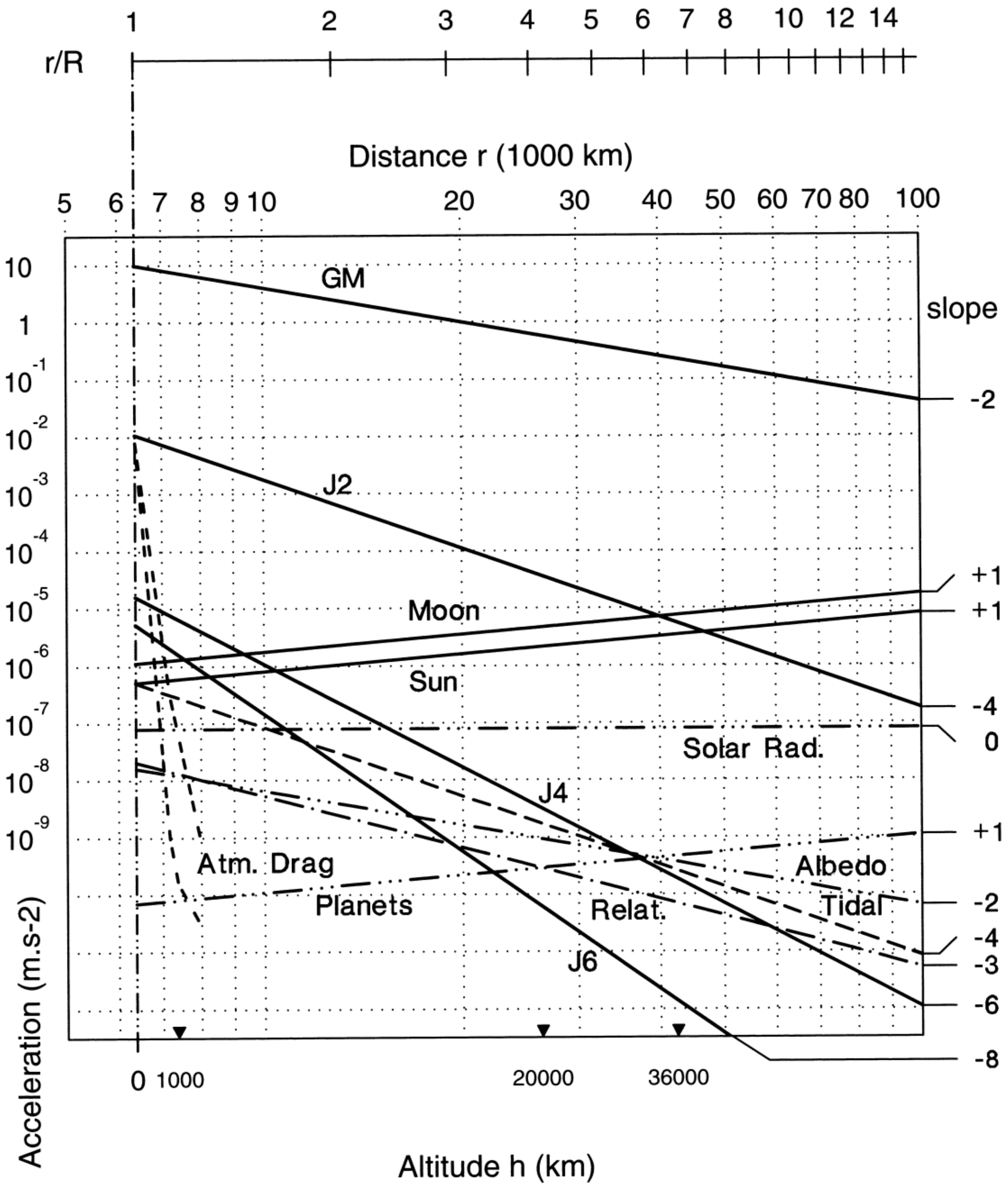

Drifts from sun-synchronous EOS-Terra satellite

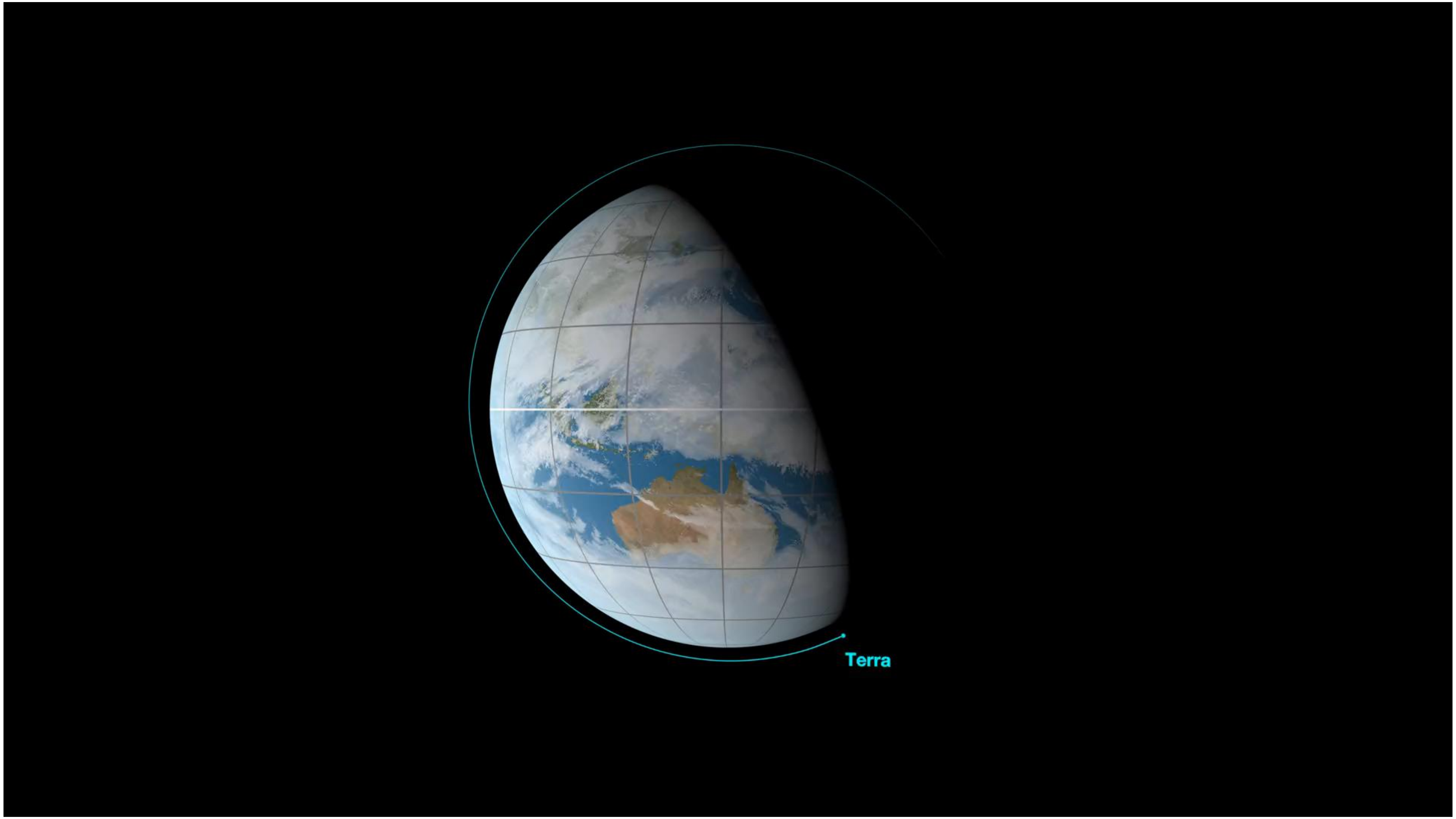

Drifts from sun-synchronous NOAA satellites

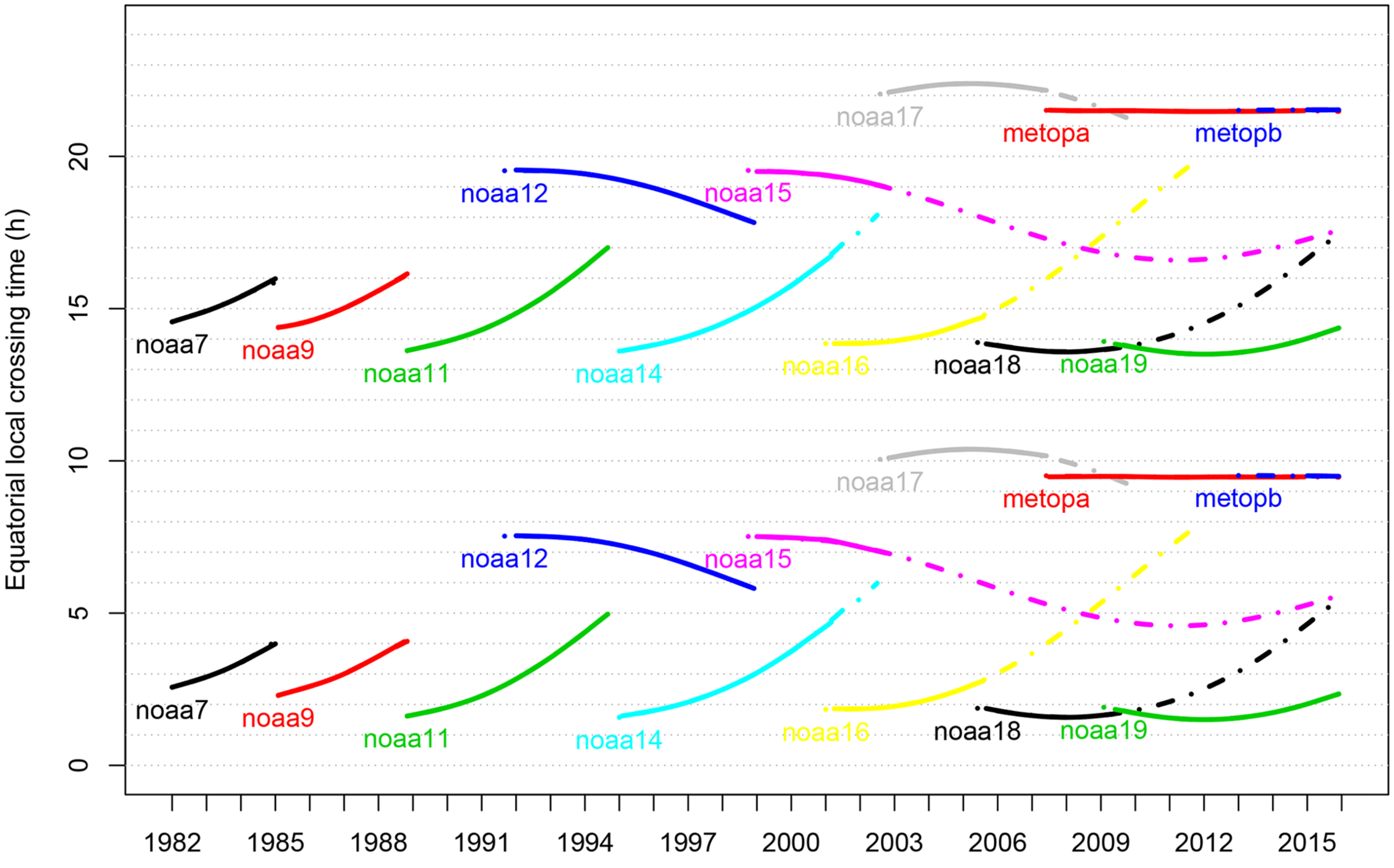

Time series of equatorial crossing time of the NOAA and MetOp satellites.
Two observations per time per satellite are related to two satellite nodes (ascending and descending). The dot-dashed lines indicate data which are included in the CLARA-A2 dataset but excluded in other CFC CDR (e.g. the Cloud_cci dataset) due to an overlap with other satellites. This exemplifies one source of spurious trends in satellite CDRs caused by different data aggregation strategy.

Bojanowski et al. (2020)

Drifts from sun-synchronous NOAA satellites

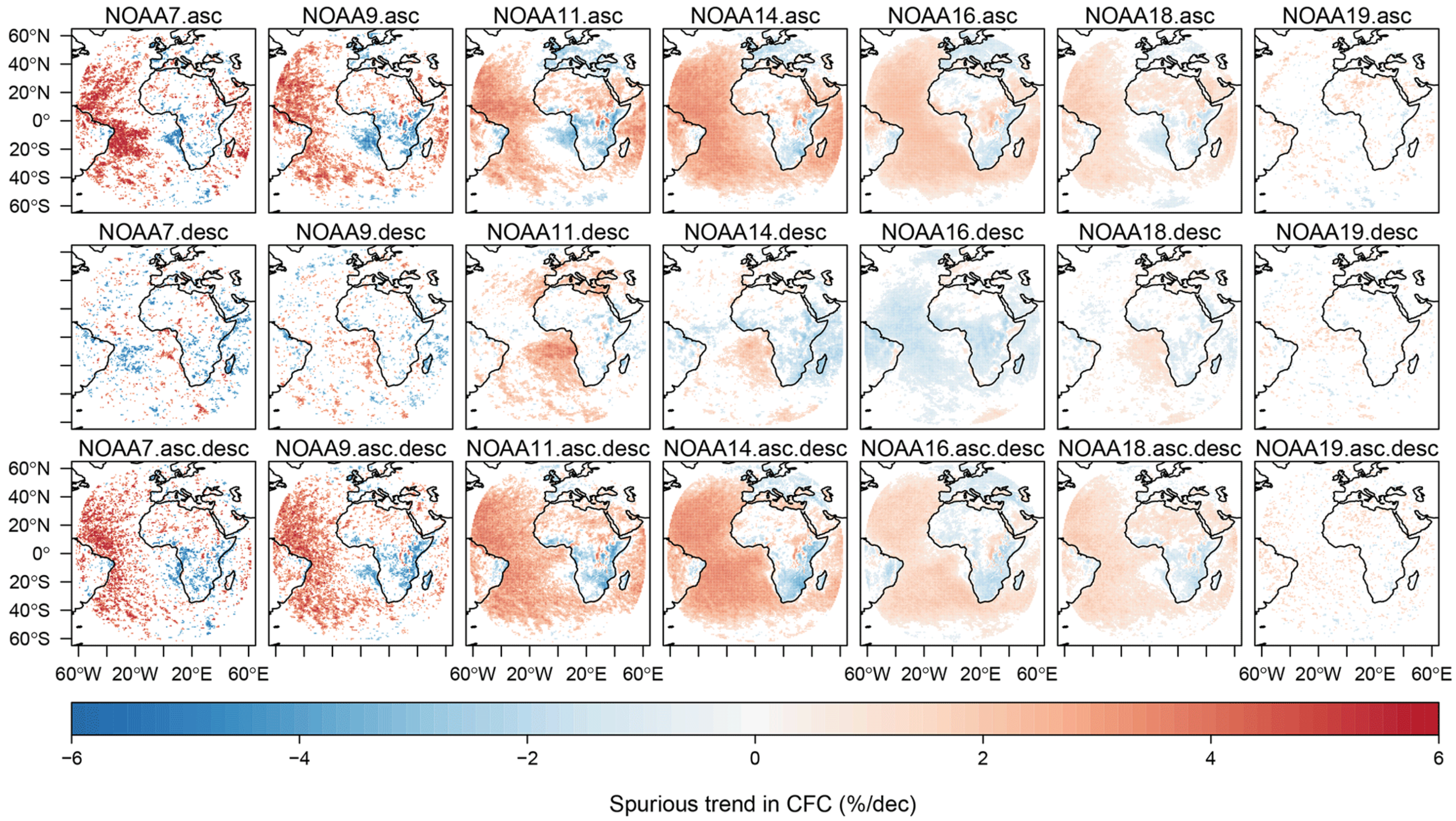

Spurious trends in CFC caused by orbital drift presented for each PM NOAA satellite and each node. Only statistically significant trends are shown.

Bojanowski et al. (2020)

Instrument calibration and impact

Instrument calibration is essential to achieve its mission objectives. In general, it can be divided into the following two categories.

Pre-launch calibration

The key objectives of pre-launch calibration include, but not limited to

(1) Evaluating sensor performance under different operating conditions that might be experienced in space;
(2) Deriving calibration parameters that are needed to support sensor on-orbit calibration and its L1B calibration algorithm;
(3) Establishing sensor calibration traceability and accuracy with reference measurements and comprehensive data analyses to help identify and quantify all contributors to the end-to-end calibration error budget.

On-orbit calibration (Onboard calibration)

The key objectives of onboard calibration include, but not limited to

(1) Ensuring data accuracy and maintain data consistency;
(2) Validating instrument performance against pre-launch specifications and detect any degradation and shifts;
(3) Identifying any gradual changes or 'drift' in instrument behavior and apply corrections to the collected data, ensuring that it remains reliable throughout the mission's duration;
(4) Providing a basis for comparing and harmonizing data from different instruments across multiple satellites or with ground-based observation systems.
(5) Enabling the integration of data from multiple sources by ensuring that each dataset is calibrated to a common standard.

Instrument calibration and impact – example

Blackbody OBC -> mid- and long-wave infrared bands (3.5 μm ~ 14.4 μm)
SD OBC -> visible, near infrared bands (0.4 μm ~ 2.2 μm)

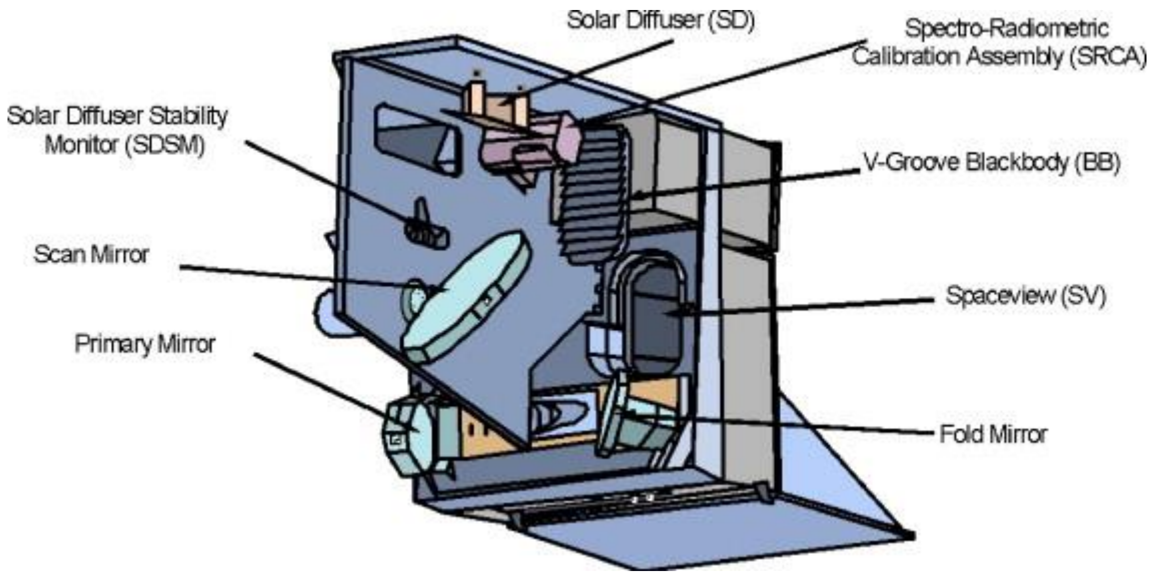

SD – Solar Diffuser
SDSM – Solar Diffuser Stability Monitor
SRCA – Spectroradiometric Calibration Assembly

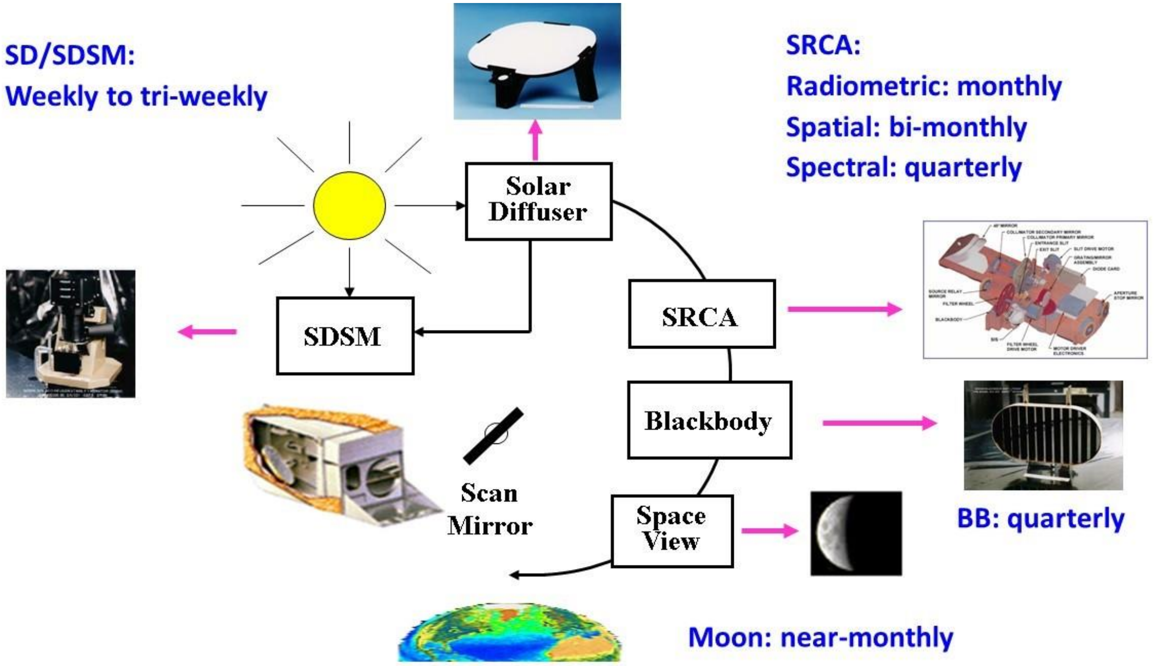

Schematic of MODIS on-orbit calibration and characterization approaches and nominal scheduling frequencies.

Xiong and Butler (2020)

Instrument calibration and impact – example

Summary of Terra MODIS L1B data collections and key calibration updates.

MODIS Collection	Time range	Improvements
Collection 2	03/2000–05/2001	Improvement of SWIR Crosstalk Correction Algorithm; <DN_SV> Computation When Moon is in SV Port for TEB.
Collection 3	05/2001–01/2003	Piecewise linear time dependent LUT implemented; <DN_SV> computation when Moon is in SV port for RSB.
Collection 4	01/2003–04/2007	Band 26 correction using band 5; time dependent RVS for bands 3, 8, and 9 using SD, lunar and SRCA gains.
Collection 5	03/2005–03/2017	Detector-dependent SWIR cross-talk correction, mirror-side dependent band 21 calibration; pitch maneuver derived RVS for TEB; time-dependent RSB RVS was extended to bands 1-4, 8-12, 17-19, using SD, lunar, and EV mirror-side ratios; mirror side 2 RSB RVS are normalized to mirror side 1.
Collection 6	11/2012–present	RSB RVS changed to quartic from quadratic; improved uncertainty algorithm for both RSB and TEB; TEB a0/a2 LUTs derived from BB cool-down data; EV-based RVS for bands 1-4, 8-10; correction for SD degradation at 936 nm (SDSM D9) and beyond; detector dependent RVS for bands 3, 8-12; SWIR sending band switched from 28 to 25.
Collection 6.1	09/2017–present	Crosstalk correction algorithm applied to LWIR PV bands (27-30); QA LUT updated due to changes made; SWIR sending band switched from 28 to 25.

Xiong and Butler (2020)

Instrument calibration and impact – example

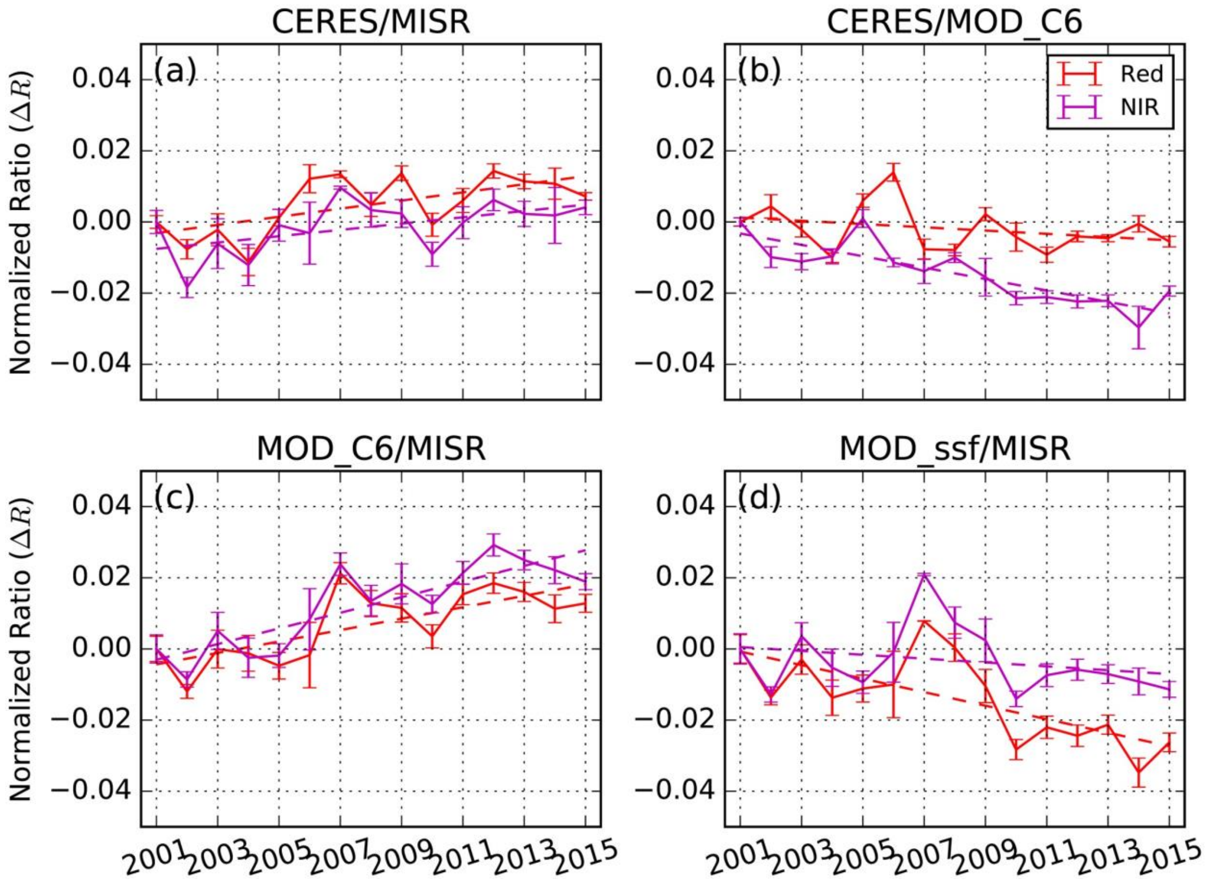

Greenland Spot case of normalized radiance ratio trends for successive Aprils, for (a) CERES against MISR, (b) CERES against MODIS Collection 6, (c) MODIS Collection 6 against MISR, and (d) MODIS SSF against MISR. Data were limited to 0.07 ≤ PWC ≤ 0.12 cm.

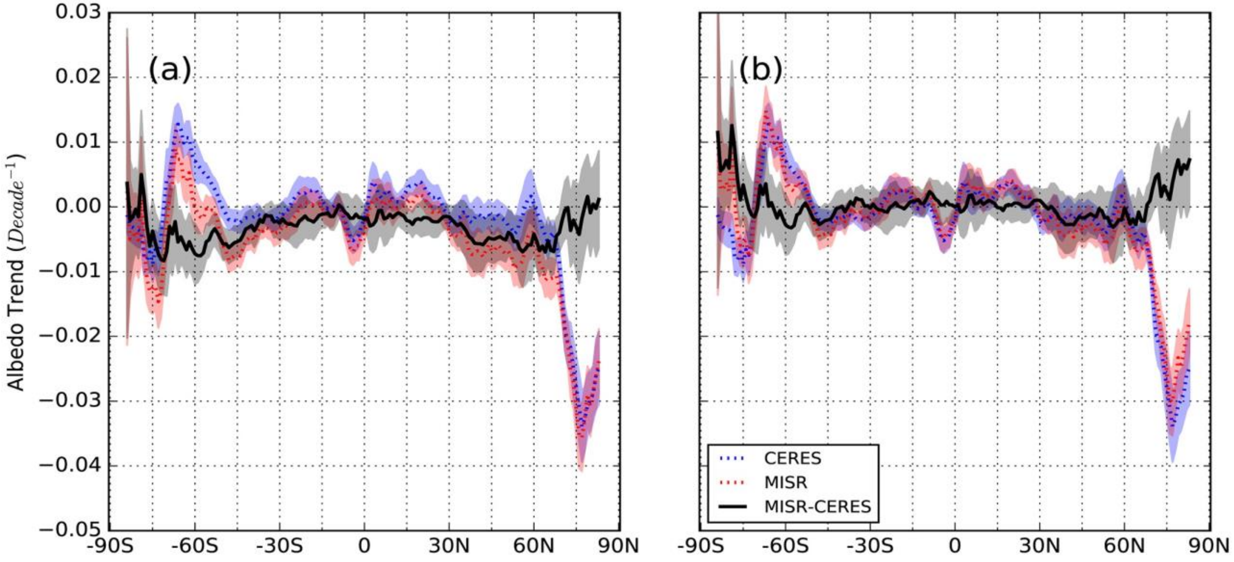

Latitudinal decadal trend of TOA albedo, (a) before and (b) after applying a correction coefficient of +1% decade−1 for CERES-MISR intercalibration.

Zhan et al., (2016)